JOURNAL OF APPLIED ELECTROCHEMISTRY 19 (1989) 519–530

Ni and Mo coatings as hydrogen cathodes

J. DIVISEK, H. SCHMITZ

Institute of Applied Physical Chemistry, Nuclear Research Centre (KFA) Jülich, P.O. Box 1913, D-5170 Jülich, FRG

J. BALEJ

Consultant Bureau for Chemical Engineering, D-5170 Jülich, FRG

Received 20 September 1988; revised 8 January 1989

The catalytic activity of hydrogen cathodes based on Ni/Mo coatings prepared in different ways has been investigated under conditions of advanced alkaline water electrolysis in 10 M KOH at 100° C, in the current density range 0.05–1.0 A cm^{-2}. The activity of electrodeposited Ni/Mo and Ni/Mo/V coatings was quite low, apparently due to their low effective surface area. The activity of all thermally deposited Ni/Mo coatings, electrodeposited Ni/Mo/Cd coatings and of Raney nickel–Mo alloys has been found to be high. When accompanied by some current interruptions of various durations, however, it successively decreased during long-time electrolysis, especially when the residual potential of the electrode, after the current interruption, approached a certain threshold value. The rate of electrode deactivation depends on its mode of preparation as well as on electrolysis conditions, particularly on conditions during the current interruptions. The Mo content in the coating decreased quickly by a factor of 2–10 under operating conditions. The deactivation of the electrodes could be expressed as an increase in the absolute values of both Tafel constants. The addition of Mo to the Raney nickel improves its catalytic efficiency as long as Mo is not dissolved. The enhancing of catalytic activity by Mo in Raney nickel is partly caused by synergetic effects between Ni and Mo, as follows from their electronic structure, and partly by material stabilization as follows from comparison with the Raney nickel (Zn).

1. Introduction

With the aim of reducing the cell voltage in advanced alkaline water electrolysis, a series of catalytic materials for anodes as well as for cathodes has been proposed and examined. A survey of the activity of various electrocatalysts for anodic oxygen evolution under comparable conditions (10 M KOH, 100° C, j_a = 0.1–1.0 A cm^{-2}) has recently been published [1]. The lowest oxygen overvoltage was observed for Raney nickel electrodes made by the KFA technique [2], their activity remaining unchanged for more than 13 000 h [3]. A review of anode materials for alkaline water electrolysis has been presented by Hall [4].

Raney nickel electrodes made by the KFA technique have also proved to be very effective hydrogen cathodes [2, 3]. Generally, good catalytic activity for hydrogen evolution from alkaline solutions has been found for some combined coatings on the basis of Ni (and/or Co) with Mo (and/or W, V, etc.). The hydrogen overvoltage on compact molybdenum and tungsten in acidic [5], as well as basic, solutions [6] is higher than on compact nickel. However, it is well known that even very low amounts of Mo (6+), as well as W (6+), Cr (6+), V (5+), etc. in the brine cause a sharp decrease of hydrogen overvoltage on sodium or potassium amalgam cathodes during chlor-alkali electrolysis by the amalgam process (e.g. [7]). This fact has been used for an '*in situ*' activation of amalgam decomposers by Mo (6+) salts [8, 9]. The '*in situ*' activation of less active or deactivated hydrogen cathodes by low amounts of soluble salts of Mo (6+) and/or Co(Ni) (2+) [10, 11] is based on the same principle.

There are various proposals for the preparation of hydrogen cathodes with catalytic coatings on the basis of Ni (or Co, Fe) with Mo (or W, V): electrolytic [11–15], electrophoretic [16] or currentless deposition [17], flame [18, 19] or plasma spraying [19, 20], sintering of metal powders [21] or other techniques using metallic materials [22], or thermal decomposition of decomposable substances to mixed oxides with their subsequent reduction to metal alloys [19, 23–29].

The hydrogen overvoltage on such electrodes is mostly very low. Appleby and co-workers [25] gave, e.g. 75 mV at 0.4 A cm^{-2} in 34 w/o KOH at 90° C on a freshly prepared cobalt molybdenum electrode. According to Brown *et al.* [19, 26–29], the hydrogen overvoltage was in the range of 70–90 mV at a current density of 1 A cm^{-2} in approx. 30 w/o KOH at 70° C, with the Tafel slope b = 40–45 mV dec^{-1} j_c, and also b = 62 mV dec^{-1} j_c according to [27], in the current density range of 0.1–1.0 A cm^{-2}. The time stability of such electrodes is good under conditions of continuous current loading (e.g. nickel substrate coated with

0021-891X/89 $03.00 + .12

the Ni + Mo electrocatalyst was found to exhibit overvoltages between 60 and 80 mV at 0.5 A cm^{-2} for 10 000 h in 30 w/o KOH at 70° C [29]). However, the current interruptions, especially for more than 2 weeks [28], cause a profound deactivation of such electrodes.

Conway *et al.* [30, 31] emphasized the low values of the Tafel b constant in the range of 30–38 mV dec^{-1} j_c for the low current densities (up to approximately 0.1 A cm^{-2}) at 95° C, while for higher current densities they found b = 110–125 mV dec^{-1} j_c, for Ni + Mo + Cd electroplated coating.

These materials have also been proposed as non-noble catalysts for hydrogen ionization in fuel cells [32, 34], however their activity was not sufficiently stable with time. As the work of Brown *et al.* [29] showed, the catalytic activity of Ni + Mo coatings decreases after anodic polarization to potentials more positive than 120 mV (RHE).

The explanation of the catalytic activity of the mixed coatings on the basis of Ni + Mo (or similar combinations such as Co + Mo, Ni + V, etc., sometimes in polycomponent combinations such as Ni + Mo + Cd, Ni + Mo + V, etc.) has not yet been agreed upon. Conway *et al.* [30] attributed the catalytic activity of such coatings to the facilitated nickel hydride formation which enhances the hydrogen evolution rate by a corrosion mechanism. The same mechanism can also be applied, according to Conway *et al.* [30], for Raney nickel electrodes. Jaksic [35] explains the catalytic activity of these materials by the synergetic effect of both the main metallic components of the coatings belonging to the d-metal series: a well-pronounced synergism could be achieved by alloying of the transition metals which have empty or half-filled vacant d-orbitals (Ti, Zr, Mo, Hf, W) with metals of the right half of the transition series, which have internally paired d-electrons (Fe, Co, Ni).

Other authors (e.g. [15]), however, classify molybdenum (and similarly tungsten, vanadium, etc.) as components which are leached out from the coatings in more concentrated solutions of alkali metal hydroxides, and release an active Raney structure of the main component (nickel or cobalt).

In order to obtain further information about such active cathode materials under comparable reaction conditions of advanced alkaline water electrolysis as in the previous case of electrocatalysts for anodic oxygen evolution [1], some measurements have been made with these coatings on the basis of Ni + Mo using various methods of preparation. The results of these experiments are the subject of the present paper.

2. Experimental details

Catalytic coatings on the basis of Ni/Mo were prepared either by electrolytic deposition of the Ni/Mo alloy or by thermal decomposition of suitable salts to mixed oxides, with their subsequent reduction by hydrogen to metal alloys at elevated temperature. Alternatively, the electrodes were prepared galvanically by embedding Ni/Mo/Al powder onto a substrate carrier according to [36].

For the electrolytic deposition of Ni + Mo a procedure according to Ernst *et al.* [37] was used. An alloy with approx. 18 w/o Mo could be obtained at j_c = 10 A dm^{-2} and 25° C from a solution of 0.3 mol $NiSO_4$, 0.2 mol Na_2MoO_4 and 0.3 mol Na-citrate in 1 dm^3 at pH = 10.5 (adjusted by NH_4OH).

An electrolytic coating of Ni/Mo/V was deposited by the procedure of Gala *et al.* [13] from a bath containing 62 g $NiSO_4 \cdot 7H_2O$, 15.3 g $Na_2MoO_4 \cdot 2H_2O$, 5 g $VOSO_4 \cdot H_2O$, 76 g Na-K-tartrate and 10 g NaCl in 1 dm^3 at pH 10.0 (adjusted by NH_4OH), j_c = 7 A dm^{-2} and 30° C.

Coatings of Ni/Mo/Cd were deposited following Stachurski *et al.* [15], or by a modification of the procedure of Conway *et al.* [30] from pyrophosphate solutions at pH 8.0 in both cases.

The Ni/Mo coatings by thermal decomposition were prepared according to Appleby and Crépy [23, 24] or Brown and Mahmood [19]. The film of an ammoniacal mixed solution of nickel nitrate and ammonium molybdate, obtained by dipping the appropriate supporting conductive material into the solution, was decomposed to the mixed oxides either under the red glow of a Bunsen burner (i.e. at 900–1000° C) [19] or at 450–550° C [23, 24] in a stream of hot air. This procedure was repeated several times until the desired thickness of the layer of mixed oxides was obtained. The subsequent reduction to metal alloy was carried out in a hydrogen stream at 450–500° C for 1–2 h [19, 23, 24]. The reduced specimens were then cooled to ambient temperature in a hydrogen or argon (both 99.999%) atmosphere.

A perforated nickel sheet (Ni 200), 0.5 mm thick, with 40% free area, served as the supporting conductive material for electrodeposited as well as thermally deposited coatings. In some cases, for thermally deposited coatings, nickel mesh screens were also used alone or with a layer of sintered nickel powder (INCO 225). As a supporting conductor for galvanically embedded catalyst powder a VECO sheet of 0.3 mm thickness with 40% free area was used.

The electrocatalytic activity of the electrodes was examined in a PTFE vessel (500 ml) with a lid, in which the working electrode (1 × 1 or 2 × 3 cm^2), the Raney nickel counter electrode in a PTFE casing with the NiO diaphragm [2], an Hg/HgO reference electrode with a PTFE Luggin capillary, a contact thermometer, water inlet and hydrogen inlet and outlet were fixed. Water consumed by electrolysis and evaporation was replaced automatically by means of a level controller. The temperature of the solution was maintained at 100 ± 1° C by means of external heating. In some cases, the polarization behaviour of larger electrodes (30 cm^2) was investigated in a model electrolyzer with a zero-gap configuration of the cathode, a Raney nickel anode and an NiO diaphragm.

The measured electrode was polarized galvanostatically with constant current density j_c = 0.4 A cm^{-2}

(standard working conditions). At certain intervals the polarization curve was measured in the range 1.0–0.05 A cm^{-2} with decreasing current density. The *IR*-free cathode potentials against an Hg/HgO reference electrode in the same solution as in the electrolytic vessel, but held at the ambient temperature (25 ± 2° C), were recorded by means of a current interrupter and storage oscilloscope (Explorer II, Nicolet Instruments). Under such conditions, the hydrogen overvoltage was computed according to the following relation [38]

$$\eta_{H_2} = E_c + 0.905 \quad (V) \qquad (1)$$

where E_c denotes the *IR*-free potential difference between the measured cathode under current flow at 100° C and the Hg/HgO reference electrode kept at 25 ± 2° C.

In all cases a 10 M KOH solution, prepared at ambient temperature from KOH p.a. (Merck) and deionized water, was used as the electrolyte. In long-time experiments, such a solution was replaced several times by a fresh one in order to eliminate the influence of gradual carbonation of the hydroxide solution.

For the preparation of Raney nickel electrodes on the basis of Ni/Mo/Al, the appropriate powder was produced. It consisted of the Ni/Al alloy with different amounts of Mo. For some purposes, small amounts of Ti were also added. The powder composition was varied according to the published literature data [22, 39, 40].

The metal powder was fixed galvanically on the carrier surface [36]. The fixation agent was cathodically deposited nickel. As an alternative, Ni/Mo/Al electrodes from Lurgi GmbH, with similar chemical composition but fixed by means of rolling techniques [41, 42], were also tested.

The composition of the further electrode coatings was either determined from the known solution composition (thermally deposited coatings) or from a chemical analysis of the galvanically deposited coatings with the use of EDAX or spectral analysis methods. In some cases a crystallographic analysis of the coating using X-ray diffractometry was also carried out.

The potential decay curves were recorded using the storage oscilloscope Explorer II (Nicolet Instruments).

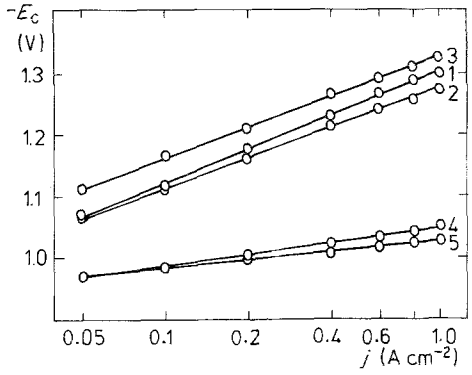

Fig. 1. Polarization curves of hydrogen evolution (vs Hg/HgO/OH$^-$ kept at 25° C) at various electrodes in 10 M KOH at 100° C and ambient pressure: (1) etched perforated Ni sheet; (2) Ni/Mo (galv.); (3) Ni/Mo/V (galv.); (4) Ni/Mo/Cd (galv. [15]) without heating; (5) Ni/Mo/Cd after heating at 275° C in air for 1 h, and 150 h of electrolysis.

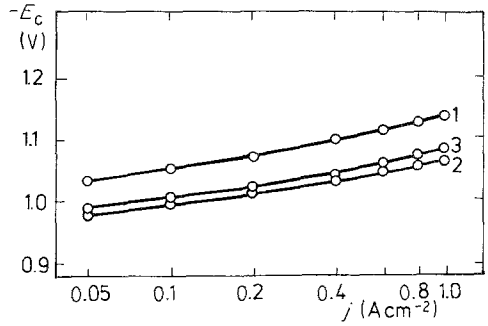

Fig. 2. Polarization curves of hydrogen evolution (vs Hg/HgO/OH$^-$ kept at 25° C) in 10 M KOH at 100° C and ambient pressure at an Ni/Mo/Cd electrode (galv. [30]): (1) without heating, after 2 h of electrolysis; after heating at 290° C in air for 1 h: (2) after 2 h and (3) 20 h of electrolysis.

3. Results and discussion

3.1. *Electrodeposited coatings*

Under the conditions given above, a coating of Ni/Mo with 21 w/o Mo of 46 mg cm^{-2} was obtained at a current efficiency of 85%. These results are in good agreement with the original data [37].

The polarization curve for hydrogen evolution on such a cathode after 20 h of electrolysis in 10 M KOH at 100° C and ambient pressure is given by curve 2 in Fig. 1. As may be seen in comparison with the polarization curves for the same reaction on pure etched perforated Ni sheet cathode (curve 1) after 20 h of electrolysis, there is little difference between the activities of the two materials.

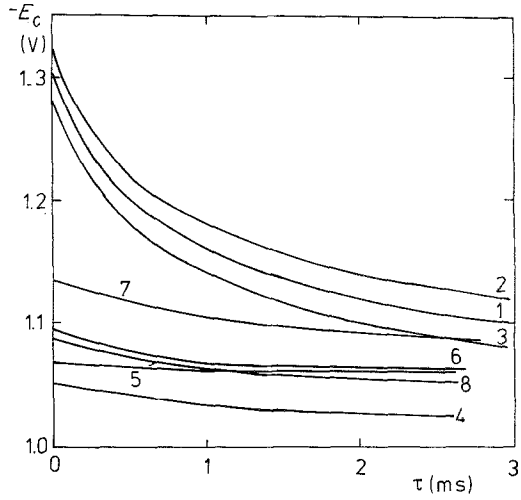

Fig. 3. Time delay of cathode potential (vs Hg/HgO/OH$^-$ kept at 25° C) after a current interruption at j_c = 1.0 A cm^{-2} in 10 M KOH at 100° C and ambient pressure for various electrodes: (1) etched perforated Ni sheet; (2) Ni/Mo (galv.); (3) Ni/Mo/V (galv.); (4) Ni/Mo/Cd (galv. [15]) without heating; (5) Ni/Mo/Cd after heating at 275° C in air for 1 h; (6) Ni/Mo/Cd after *in situ* reactivation with Mo (6+) and Fe (2+) salts; (7) Ni/Mo/Cd (galv. [30]) without heating and (8) after heating.

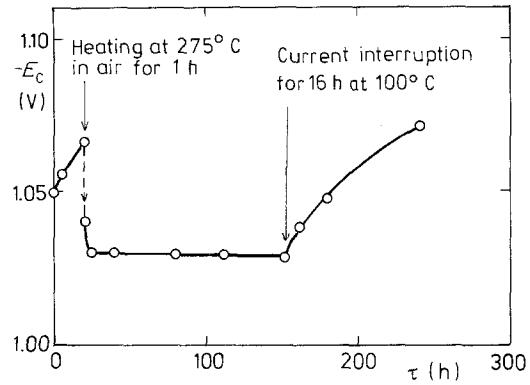

Fig. 4. Time dependence of the cathode potential (vs Hg/HgO/OH$^-$ kept at 25° C) of an Ni/Mo/Cd electrode (galv. [15]) in 10 M KOH at j_c = 1.0 A cm^{-2} and 100° C and ambient pressure, at the beginning without and then after heating in air at 275° C for 1 h, and after a current interruption for 16 h at 100° C.

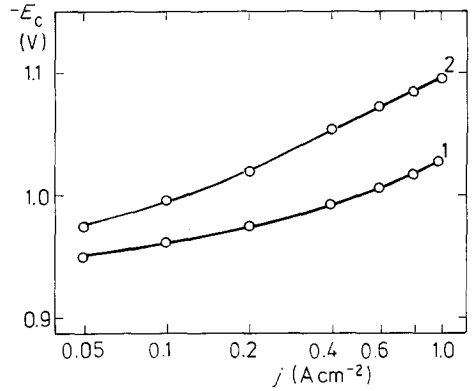

Fig. 5. Polarization curves of hydrogen evolution in 10 M KOH at 100° C and ambient pressure at an Ni/Mo cathode (thermal, approx. 900° C): (1) after 1 h; (2) after 19 h of electrolysis.

A coating of Ni/Mo/V according to [13], with 21 w/o Mo and 0.1 w/o V of 59 mg cm^{-2} also showed an activity similar to that of pure etched Ni perforated sheet cathode (curve 3 in Fig. 1).

Different results were obtained with electrodeposited coatings of Ni/Mo/Cd according to Stachurski *et al.* [15] or Conway and co-workers [30]. In the first case the coating composition according to the EDAX analysis of the surface was 45.4 w/o Ni, 49.5 w/o Mo and 5.1 w/o Cd, and in the second case 59.3 w/o Ni, 37.4 w/o Mo and 3.3 w/o Cd, respectively. The coating amount corresponded to 30 mg cm^{-2} in both cases (relative to both sides of the perforated sheet cathodes). The deposits were granular, with metallic lustre and without large cracks. The electrodes were then leached in 10 M KOH for several hours, in accordance with Stachurski's patents [15]. Such a treatment decreased the original Mo content by approximately 75%, according to the EDAX analysis. These patents also recommend a subsequent heating in air or inert atmosphere at 100–350°C for 1–2 h. The polarization curves are also given in Fig. 1.

As may be seen from this figure, the catalytic activity of Ni/Mo/Cd coatings is remarkably higher than the activity of uncoated Ni sheet or Ni coated with Ni/Mo electrodeposit only. Heating of the Ni/Mo/Cd coating at 275° C led to a further increase in the activity. Similar results were also obtained with electrodeposited coatings of Ni/Mo/Cd after Conway *et al.* [30]. As may be seen from Fig. 2, a decrease of the cathodic overpotential at j_c = 1.0 A cm^{-2} by 75 mV (measured 2 h after the beginning of the polarization) was observed. However, this activation diminishes with time, as may be seen from curve 3, measured after an additional 18 h of electrolysis.

The higher effective activity of these electrodes with Ni/Mo/Cd coatings is caused, apart from other reasons, by an increase in specific surface area, as may be deduced from a slower decay of cathodic potential after the current interruption (see curves 4–8 in Fig. 3), caused by enhanced pseudocapacity.

The behaviour of the electrocatalysts after repeated current interruptions lasting several hours or days, which is a common occurrence in industrial electrolytic processes, is very important from the practical point of view. The behaviour of thermally prepared Ni/Mo coatings in this respect is not uniform, according to various reports by Brown and Mahmood *et al.* [19, 26–29]. For electrolytic coatings there are no corresponding data in the literature yet.

As may be seen from Fig. 4, a current interruption for 16 h caused a rapid deactivation of the electrodeposited Ni/Mo/Cd coating during the subsequent electrolysis characterized by an increase in both Tafel constants, although the cathode potential immediately after switching on the current remained at the same level as before the current interruption. A trial to reactivate this electrode by an '*in situ*' activation through an addition of soluble Mo (6+) salt according to various proposals [8–11] ended, however, without any success.

3.2. *Thermally deposited coatings*

The preliminary experiments have shown that a better adhesion of the intermediate layer of mixed oxides to the conductive base may be obtained by thermal decomposition of a film of decomposable Ni + Mo salts at medium temperatures (400–500° C), according to [23, 24], than by using higher temperatures (900–1000° C) according to [19]. A worse adhesion of the coating prepared by thermal decomposition to mixed

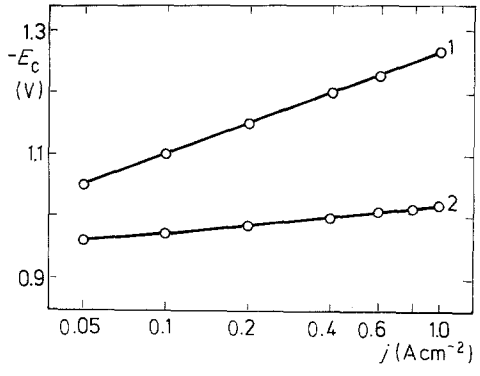

Fig. 6. Polarization curves of hydrogen evolution (vs Hg/HgO/OH$^-$ kept at 25° C) in 10 M KOH at 100° C and ambient pressure at a perforated Ni sheet electrode with (1) thermally deposited Ni and (2) Ni/Mo coating, respectively.

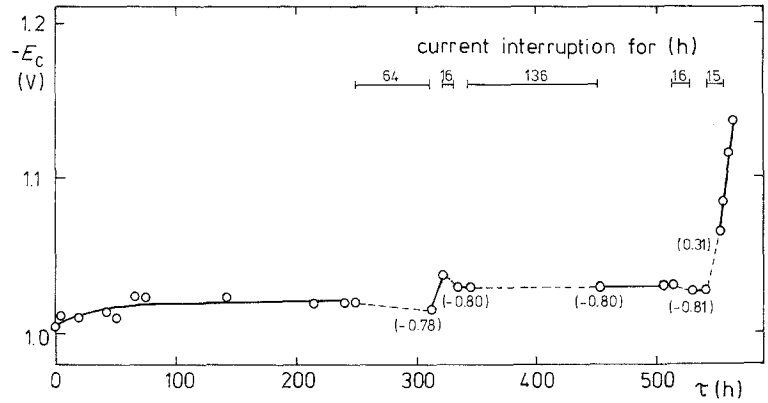

Fig. 7. Time dependence of the cathode potential (vs Hg/HgO/OH^- kept at 25° C) of an Ni/Mo cathode (thermal, 550° C, 39 mg cm^{-2}) at 1.0 A cm^{-2} in 10 M KOH at 100° C during the electrolysis with current interruptions. The numbers in parentheses denote the residual potential of the cathode at the end of current interruptions.

oxides at 900–1000° C also led to a rapid deactivation of the electrode, as may be seen from Fig. 5. The increase in the total overvoltage may probably be explained by an increase in ohmic resistance between individual particles of the layered cracked coating as well as between the former and the conductive base. Therefore, the lower decomposition temperature has commonly been used in all other preparations of electrodes of this type, because, according to [43], the decomposition of $(NH_4)_2MoO_4$ to MoO_3 proceeds in the temperature range 390–429° C. Nevertheless, also in this case the final coating of reduced metal alloy was always obtained in the form of a cracked layered deposit, as reported by Brown *et al.* [27] for coatings prepared by thermal decomposition at temperatures of about 1000° C.

In all cases, thermally deposited Ni/Mo coatings with an original content of 33 mol % Mo were prepared. The thickness of the coating was in the range 14–60 mg cm^{-2}. All thermally coated Ni/Mo electrode samples were very active at the beginning, their initial cathode potential being in the range 985–1020 mV vs Hg/HgO at 1.0 A cm^{-2}. The current density was related to the geometric area of the electrode. The polarization curves in the range 0.05–1.0 A cm^{-2} did not often obey the Tafel relation, especially at current densities smaller than 0.5 A cm^{-2}.

The proof of a catalytic effect of the mixed Ni/Mo coating can be seen from Fig. 6, representing the comparison of the polarization curves of hydrogen evolution on an electrode with thermally deposited Ni/Mo coating (curve 2) and on an electrode coated solely with a layer of metallic nickel prepared by thermal decomposition of a $Ni(NO_3)_2$ film under similar conditions (curve 1).

Great attention has been paid to the time stability of the catalytic activity of thermally deposited Ni/Mo coatings, especially in combination with current interruptions.

Figure 7 depicts results of measurements with an electrode during current interruptions either without short circuiting (first four interruptions), or the cathode short circuited with an anode having a lower pseudocapacity. The numbers in parentheses in Fig. 7 denote the cathode residual potentials at the end of the current interruption. As may be seen, the activity

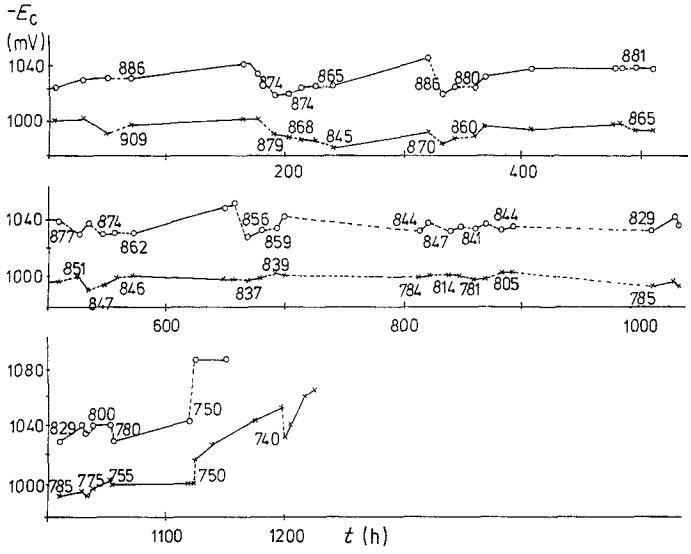

Fig. 8. Time dependence of the cathode potentials (vs Hg/HgO/OH^- kept at 25° C) of an Ni/Mo (thermal, 550° C, 40 mg cm^{-2}) (×) and a Raney nickel cathode (○), at 0.4 A cm^{-2} in 10 M KOH at 100° C, with some current interruptions. The numbers denote the residual potential of the electrode at the end of the current interruption.

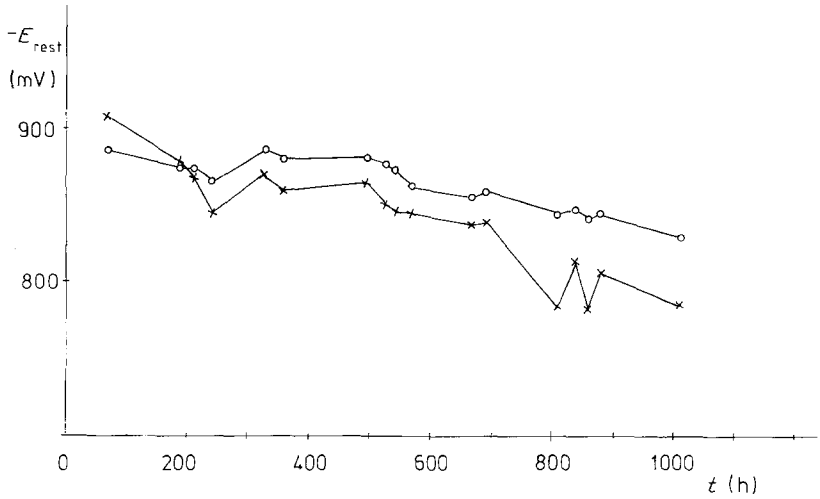

Fig. 9. Time dependence of the rest potentials of the Ni/Mo and Raney nickel cathodes.

of the cathode remained practically unchanged after current interruptions lasting some days if its potential did not reach too positive values. In the case where the cathode was short circuited with an anode having higher pseudocapacity (last current interruption in Fig. 7), a sharp deactivation of the cathode was observed. This sharp deactivation was caused by an approach of the cathode residual potential to the reversible potential of the oxygen anode for some time during short circuiting of the cathode with the Raney nickel anode with higher pseudocapacity. An '*in situ*' reactivation by the addition of Mo (6+) ions failed, as in the previous case.

In another experiment a cathode with thermally deposited Ni/Mo coating and a Raney nickel cathode on the Ni/Zn basis [2], with 40 mg cm^{-2} of active coating in both cases, were compared with respect to the electrocatalytic stability under identical operation conditions in 10 M KOH at 100° C. Both electrolyzers were connected in series. In the first part of this investigation, lasting about 1000 h, the electrolysis at j_c = 0.4 A cm^{-2} was periodically interrupted and the cathodes were short circuited with the appropriate anodes having lower pseudocapacities than the former ones. The experimental points in Fig. 8 denote the cathode potentials (vs Hg/HgO in 10 M KOH at room temperature) of examined electrodes at the given time for j_c = 0.4 A cm^{-2}. The residual potentials (on the same scale) at the end of current interruptions are given at each corresponding point. As is seen from Fig. 8 the electrocatalytic activity of both electrodes during these operating conditions remained practically unchanged.

In contrast to the practically constant potential values of both electrodes during the electrolysis at the current density of 0.4 A cm^{-2}, the rest potentials of these electrodes, measured at the end of individual current interruptions, decreased almost continually with the time of electrolysis (see Fig. 9). Only at the beginning of these interruption experiments, after prolonged cathodic polarization, a practically original state of electrode properties was restored, leading almost to the original values of the rest potentials. The slower decrease of the rest potential of the Ni/Zn cathode may be attributed to its higher pseudocapacitance in comparison with the Ni/Mo electrode.

It may be concluded from the results of this part of the investigation that a decrease of the rest potential to −820 mV vs Hg/HgO (i.e. to +85 mV vs RHE) for the Raney nickel electrode on the Ni/Zn basis as well as to −780 mV vs Hg/HgO (i.e. +125 mV vs RHE) for Ni/Mo does not cause any decrease of the electrocatalytic activity of both active materials to the cathodic hydrogen evolution.

In the second part of the experiment (1000–1200 h in Fig. 8) the examined electrodes were potentiostatically polarized to gradually more positive potentials after their previous stationary cathodic polarization at j_c = 0.4 A cm^{-2} in 10 M KOH at 100° C and ambient pressure.

After each potentiostatic polarization the electrodes were again cathodically polarized at j_c = 0.4 A cm^{-2}

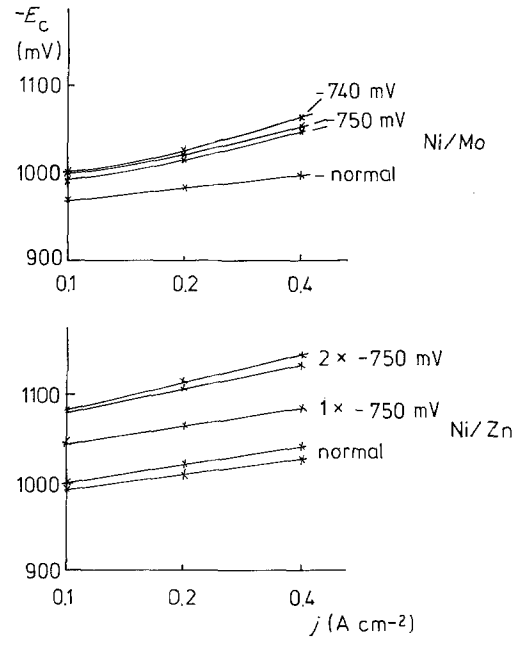

Fig. 10. Polarization curves of Ni/Mo and Ni/Zn cathodes under normal working conditions and after their depolarization to −750 mV Hg/HgO reference electrode.

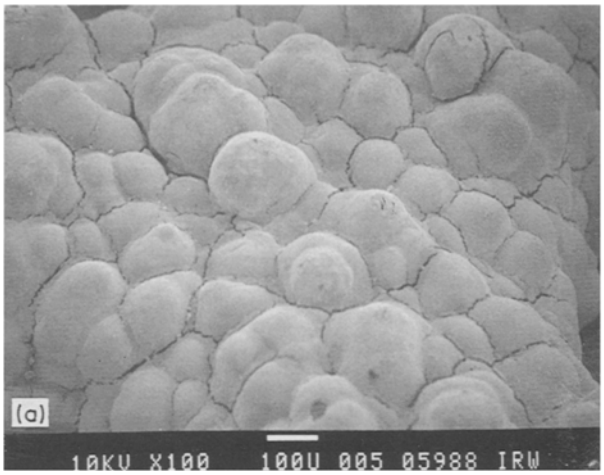

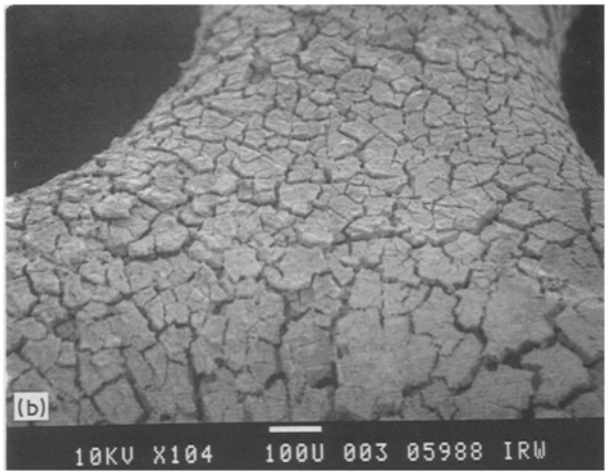

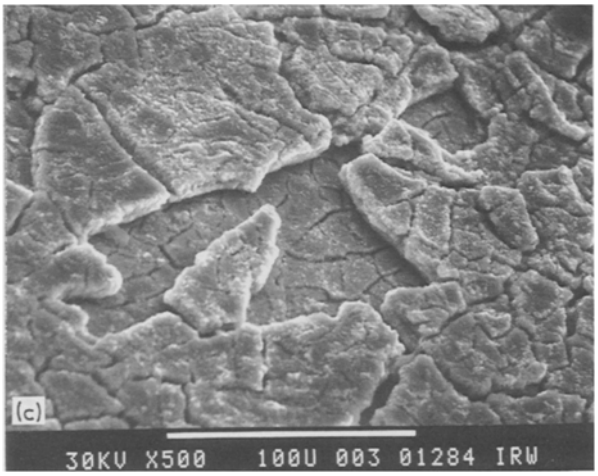

Fig. 11. Surface of the Ni/Mo electrode and Ni/Zn after electrolysis. (a) Raney nickel (Zn); (b) Ni/Mo electrode; (c) scaled Ni/Mo electrode.

for several hours and their cathodic potential was measured as a function of time. On the basis of these results it may be concluded that the electrocatalytic activity of the Raney nickel cathode on the Ni/Zn basis remained practically unchanged until the potential of this electrode, during the subsequent current interruption followed by potentiostatic polarization, reached the value of -750 mV vs Hg/HgO (i.e. $+155$ mV vs RHE). After potentiostatic polarization at $E = -750$ mV (Hg/HgO) for 60 min the potential of this electrode, after 15 h of subsequent cathodic polarization at $j_c = 0.4\,A\,cm^{-2}$, rose to -1084 mV (i.e. $\eta_{H_2} = -180$ mV) and, after a further 24 h at the same conditions, to -1130 mV vs Hg/HgO (i.e. $\eta_{H_2} = -225$ mV). At this stage, further observation of the electrode was stopped.

Similar results were also observed for the Ni/Mo electrode. At potentiostatic polarization at potentials more negative than -750 mV vs Hg/HgO, no decrease of the electrocatalytic activity for cathodic hydrogen evolution was observed. Only polarization at $E = -750$ mV vs Hg/HgO for 60 min led to the first elevation of hydrogen overvoltage by approx. 40 mV, after subsequent cathodic polarization at $j_c = 0.4\,A\,cm^{-2}$ for 15 h, and by a further 10 mV after a further 24 h at the same conditions. Subsequent potentiostatic polarization at -740 mV vs Hg/HgO (i.e. $+165$ mV vs RHE) for 90 min and further cathodic polarization at $j_c = 0.4\,A\,cm^{-2}$ for 25 h led to a shift of the cathode potential to $E_c = -1065$ mV vs Hg/HgO (i.e. $\eta_{H_2} = -160$ mV). It may therefore be concluded that the same critical potential $E = -750$ mV vs Hg/HgO (i.e. $+155$ mV vs RHE) for a sufficient time (approx. 1 h) causes a distinct irreversible deactivation of both examined cathode materials for hydrogen evolution in 10 M KOH at 100° C, the deactivation of the Ni/Mo cathode proceeding probably more slowly in comparison with the deactivation rate of the Raney nickel electrode on the Ni/Zn

Table 1.

Time (h)	Rest potential Ni/Zn electrode (mV)	Electrolyte		Rest potential Ni/Mo electrode (mV)	Electrolyte	
		Ni (ppm)	Zn (ppm)		Ni (ppm)	Mo (ppm)
0	−890	0	0	−920	0	0
220	−870	< 0.5	64	−860	< 0.5	135
850	−840	< 0.5	171	−810	< 0.5	185
1080	−800 (potentiostatically)	< 0.5	325	−800 (potentiostatically)	< 0.5	198
1200	−750 (potentiostatically)	< 0.5	463	−750 (potentiostatically)	< 0.5	232
1250	−740 (potentiostatically)	< 0.5	491	−740 (potentiostatically)	< 0.5	264

Table 2.

Ni/Zn electrode (surface concentrations)			Ni/Mo electrode (surface concentrations)			
Element	Original composition (w/o)	After experiment	Element	Original composition (w/o)	Top layer after experiment (w/o)	Second top layer (w/o)
Fe	0	2.5	Fe	0	1.7	1.5
Ni	28.0	92.6	Ni	55.0	93.5	92.3
Zn	72.0	2.9	Mo	45.0	3.2	4.4
Remainder	0	2.0	Remainder	0	1.6	1.8

basis. Our findings about the decrease of catalytic activity of Ni/Mo coatings agree quite well with the findings of Brown *et al.* [29] concerning the decrease of catalytic activity of such coatings after anodic polarization to potentials more positive than 120 mV vs RHE in 30 w/o KOH (i.e. 6.9 M KOH) at 70° C.

The deactivation of the Raney (Ni/Zn) electrode used was accompanied by a distinct increase in the Tafel constant *a* and only a small increase in the Tafel constant *b*. The small ohmic polarization combined with the charge transfer overpotential remained practically unchanged (see Fig. 10).

In contrast to the former case, the deactivation of the Ni/Mo cathode was accompanied by a less marked increase in the Tafel constant *a* but by a large increase in the resistance (ohmic) polarization, not allowing a more exact determination of the corresponding value of the constant *b* (see Fig. 10).

In accordance with these findings, the micrographs of both electrodes used after all these electrochemical investigations showed no visible destruction of the surface structure of the Raney (Ni/Zn) cathode (Fig. 11a), while in the case of the Ni/Mo cathode, a distinct loosening of the original 'mudcracked' layer [27] was observed (Fig. 11b) which could easily be wiped off with the fingers.

During the experiment the samples of both electrolytes were analyzed, as shown in Table 1. A gradual rise in the two metal concentrations, Mo and Zn, parallel to the rise in the respective corresponding rest potential of the electrode, can be clearly seen from the table. After completing the experiment, the electrodes were analyzed by means of EDAX. The values given in Table 2 show that both Mo and Zn are dissolved out of the respective electrode. This corresponds to their accumulation found in the electrolyte (Table 1).

By balancing the Mo it was, for example, established that 80% of the initial quantity was present in the electrolyte and only 20% of the original content remained in the electrode.

Two locations are visible on the surface of the Ni/Mo electrode in Fig. 11b where the upper catalyst layer has peeled off. Since this location was originally lower than the upper layer, its exposure time with respect to electrolyte action is shorter than for the upper layers. Analogous to this, the EDAX analysis shows that the residual molybdenum content is also slightly higher (Table 2). In order to make this difference clearer, a new electrode was manufactured with a scaled structure (Fig. 11c) and loaded by the electrolysis as described above.

The original composition of the Ni/Mo electrode corresponded to the Ni : Mo atomic ratio of 2 : 1. After the experiment the EDAX analysis was undertaken. The electrode had a scaled structure (Fig. 11c). The upper layers showed a tendency to peel off. The spot analysis of both top layers is shown in Table 3. In the last column of the table the corresponding metal concentration in the electrolyte is shown. The table shows clearly that the Mo has been leached out from the cathode, preferably out of the top layers, and has accumulated in the electrolyte solution.

3.3. *Mo-activated Raney nickel*

In the case of Mo-activated Raney nickel, there are two characteristic manufacturing processes for large-surface electrodes, namely the rolling technique described in [41] and galvanic fixation from the nickel bath, described in [36]. In both cases a catalytically active porous structure is obtained characterized by the fact that the catalyst grains are enclosed in a 'cage' of pure nickel (Fig. 12).

Both electrode types behave practically identically. The experimental results may therefore be valid as typical values for both.

Table 3.

Element	Original composition (w/o)	Second upper layer (w/o)	Top layer (w/o)	Electrolyte content (ppm)
Cr	0	6.7	10.1	18.0
Fe	0	10.0	14.4	18.7
Mo	45.0	9.6	6.8	113.5
Ni	55.0	71.4	65.7	0
Remainder	0	2.3	3.0	–

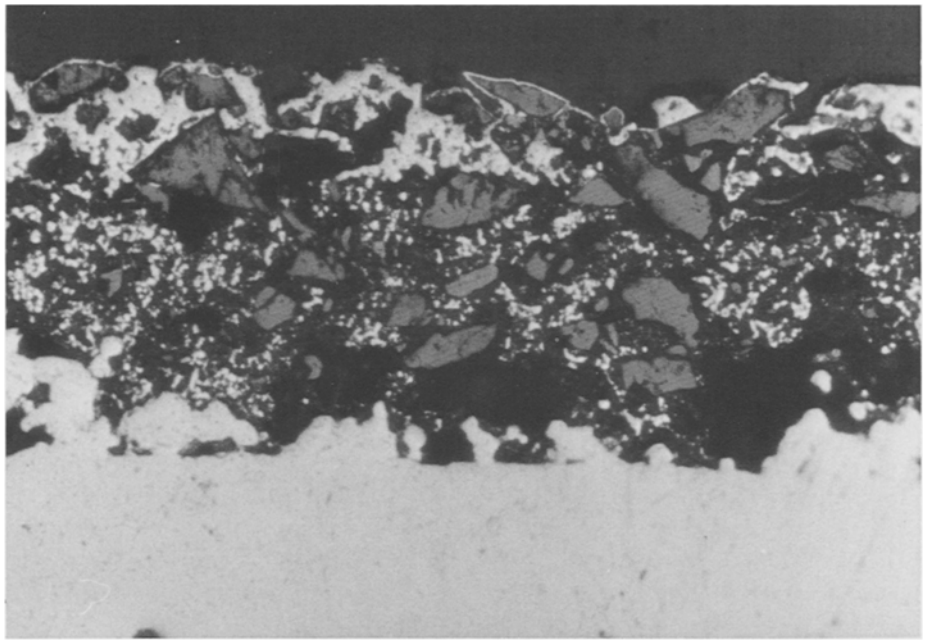

Fig. 12. Microphoto of the Mo-activated Raney nickel cathode after galvanic fixation from nickel bath and activation (200 ×).

A comparison of characteristic data between a Raney nickel electrode of the Ni–Al type alloyed with Mo and two unalloyed Raney nickel electrodes produced according to different processes is shown in Fig. 13: the first was made of Ni/Zn and the second of Ni/Al alloy. The manufacturing conditions of the latter were identical to those of Raney nickel + Mo and the only difference was the composition of the active phase (cf. Table 4). (The manufacturing technique is described in detail in [36].)

As can be seen from Fig. 13, the alloy additives (Mo + Ti) produce an improvement in the H_2 overvoltage by at least 20–30 mV in comparison to unalloyed Raney nickel.

In addition to improving the overvoltage, the presence of Mo also causes a limited increase in the depolarization stability of the Raney nickel electrodes. This is demonstrated by Figs 14–16. A typical situation after switching off the polarization current in a bipolar electrolyzer was simulated by an external short circuit between the anode and cathode [44] as shown in Fig. 14. The cathode potential rises to the value of the oxidation $Ni \longrightarrow Ni^{2+} + 2e^-$ and remains almost stationary there since the corresponding pseudocapacity must first be charged there (cf. Fig. 15). Immediately after the first rise in cathode potential to −750 mV vs Hg/HgO caused by depolarization, the position of the working potential of the Raney nickel (Al) electrode deteriorated from −1000 mV to −1025 mV vs Hg/HgO at j_c = 0.4 A cm^{-2}. After the second short circuit it actually rose to −1040 mV (cf. Fig. 16).

In the case of a Raney nickel (Al) electrode alloyed with 5% Mo, but with otherwise the same compo-

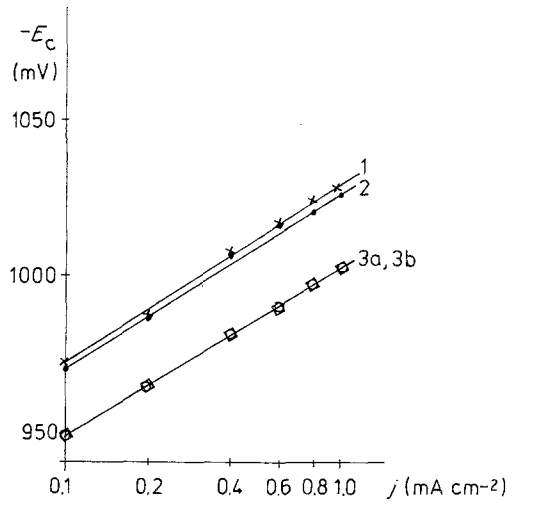

Fig. 13. Polarization curves of hydrogen evolution at various electrodes in 10 M KOH at 100° C and ambient pressure. (1) Raney nickel from Ni/Zn alloy; (2) Raney nickel from Ni/Al alloy; (3a) Raney nickel + Mo alloy; (3b) Raney nickel + Mo + Ti alloy.

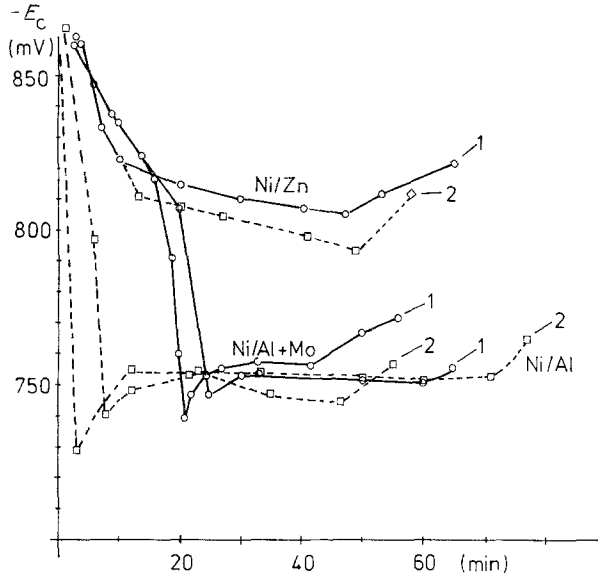

Fig. 14. Short circuit behaviour of the Raney cathode. (1) First short circuit; (2) second short circuit.

Table 4. Composition of active phase of examined Raney nickel electrodes

Electrode no.	1	2	3a	3b
Carrier coating ($mg\,cm^{-2}$)	70	50	50	50
Composition of the active fraction (w/o)	70/30 Zn/Ni	50/50 Ni/Al	50/45 Ni/Al	48/45 Ni/Al
Phase composition		$NiAl_3 + Ni_2Al_3$	$NiAl_3 + Ni_2Al_3$	$NiAl_3 + Ni_2Al_3$
Alloy addition Mo/Ti (w/o)	0/0	0/0	5/0	5/2

sition, the working potential remains stable after two short circuits at a value of −980 mV. Similar potential stability was achieved by Raney nickel (Zn), since the critical deactivation potential (approx. −750 mV) has not been reached.

The long-time effect of molybdenum on the Raney nickel electrodes was observed in another currentless test, so that it was also possible at the same time to balance the concentrations of the individual components.

It was also intended to examine the influence of Ti. For this reason, an electrode of composition 17.3% Al, 2.5% Mo, 1.2% Fe, 79.0% Ni and 0.24% Ti was exposed to a leaching effect in the currentless state in 10 M KOH at 100° C. The course of the rest potential and the concentrations of the alloying additives found in the alkaline solution (Al, Mo, Fe) are shown in Figs 17 and 18. Figure 19 shows the working potential of the electrode at three different current densities (0.1, 0.4 and 1.0 $A\,cm^{-2}$) as a function of time. Both figures clearly show that, due to the initial activation in the alkaline solution Al, Mo and Fe immediately begin to dissolve. While the Fe content in the KOH solution remains constant, Al and Mo contents increase in the first 700 h, and the rest potential is shifted positively from, originally, −920 mV towards −700 mV. The activity of the electrode also gradually falls. After reaching a certain potential threshold (here approx. −740 mV) the concentration of Al and Mo increases abruptly and the catalytic activity fades rapidly. The electrode then finally has a composition of 0.7% Al, 0.6% Mo, 1.5% Fe, 97% Ni and 0.3% Ti. Balancing Al and Mo shows that these components are practically completely dissolved. The electrode also almost completely loses its pseudocapacity which drops from the initial value of 62 $A\,s\,cm^{-2}$ to 1.6 $A\,s\,cm^{-2}$.

As shown by the electrode analysis, Ti remains in the electrode even after the latter has already lost its activity.

The increased electrode activity is therefore quite clearly connected with the presence of Mo and not with Ti, as had also been assumed [40]. There is, therefore, a clear synergetic Ni + Mo effect [35]. However, this alone is, apparently, not the only reason for good catalytic effectiveness. As the experiments with the Ni/Zn alloy show [44], the presence of a relatively large residual concentration of Zn in the Raney nickel cathode also causes good catalytic effectiveness, even though Zn is not a d-metal but, on the contrary, an sp-metal with a fully developed d-orbital. Zn behaves similarly to Mo; if due to the unfavorable (i.e. too positive) potential position of the electrode the residual zinc content is removed from the electrode then the cathode activity falls [44]. The pseudocapacity also decreases in this case, as with Mo. According to this the stabilization effect of the

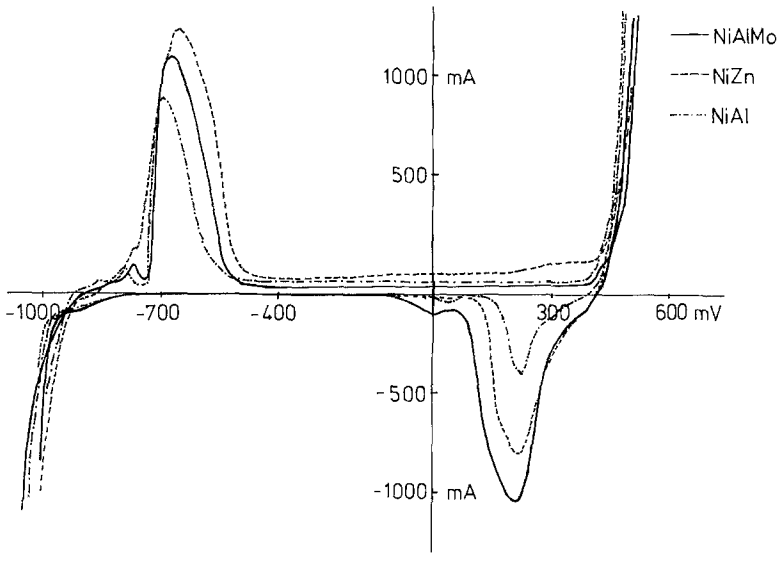

Fig. 15. Cyclic voltammogram of Raney nickel in 10 M at 100° C. (1) Raney nickel (Al); (2) Raney nickel (Zn); (3) Raney nickel (Al + Mo).

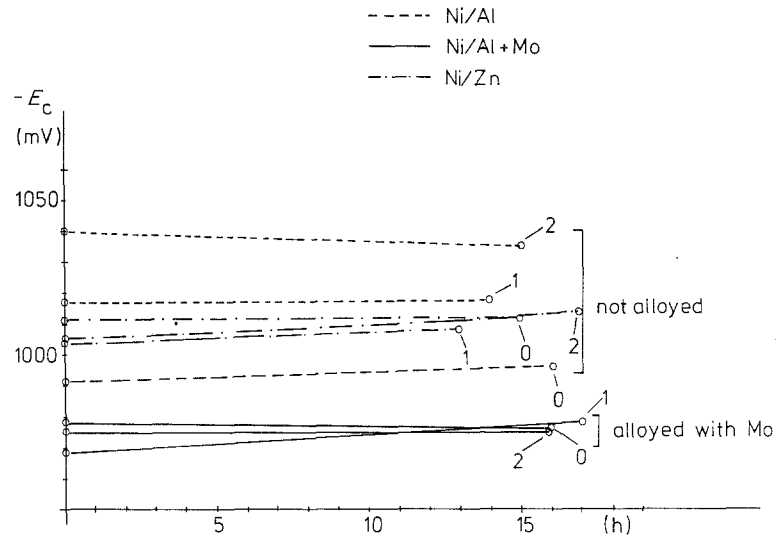

Fig. 16. Working potential of Raney cathodes after short circuiting them: (0) before the short circuit; (1) first short circuit; (2) second short circuit.

disturbed Ni structure of the Raney nickel, by the addition of Mo or Zn as an alloy, seems to play an important role, additionally coupled with the ability to form hydrides [30].

3.4. *Influence of impurities*

In addition to an evaluation of electroactivity, measurements of the influence on the activity by Fe impurities were also carried out in concentrated KOH solutions at temperatures between 85 and 100° C. As long as the electrodes are active and the operating potential more positive than −1000 mV vs the Hg/HgO electrode, then the Fe has no influence on the electroactivity in concentrations up to 30 ppm. These findings can be substantiated by an evaluation of the Pourbaix diagram extended to higher temperatures, as will be shown in a later publication.

4. Conclusions

The data reported here show that the activity of hydrogen cathodes based on Ni/Mo coatings, either as galvanic deposits Ni/Mo/Cd [15, 30], thermal deposits Ni/Mo [19, 23–29], or as Raney nickel (Mo) alloy, is high. However, it could be deactivated in the course of long-time electrolysis accompanied by some current interruptions with the rise of the rest potential to −750 mV vs Hg/HgO (i.e. +155 mV vs RHE) or more positive.

The rate of deactivation is a function of the preparation method as well as electrolysis conditions, coating amount, duration of current interruptions and the value of the cathode residual potential attained during the current interruption. As shown by the analysis of individual cathode samples and of the electrolyte in different operating stages, the deactivation of the electrodes was always accompanied by lowering the amount of molybdenum in the coating, most frequently under 50%, in some cases even under 10% of its initial content. This finding supports the considerations of this component as leachable [15], and indicates that the synergetic effect of this metal [35] on the overall catalytic activity of the hydrogen cathode is only temporary.

The observation about Ni/Mo coating deactivation characterized by an increase in both formal Tafel constants and accompanied by successive destruction and erosion of the layered coating structure may further be explained by an increase in contact resistivity between individual particles of the corroded coating. The experimental data obtained are, however, insufficient to judge whether the observed increase in the slope of the polarization curves during deactivation has any connection with the change in

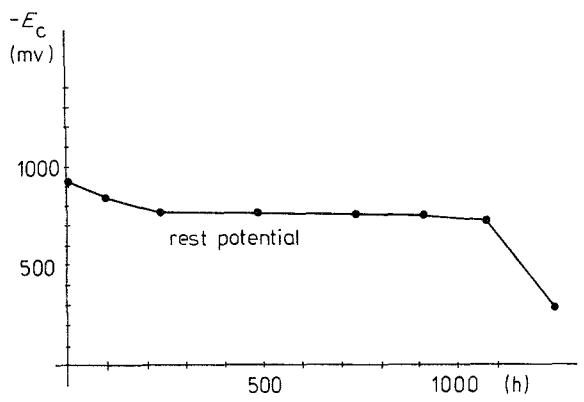

Fig. 17. Rest potential of Raney nickel, consisting of Mo + Ti alloy, as a function of time.

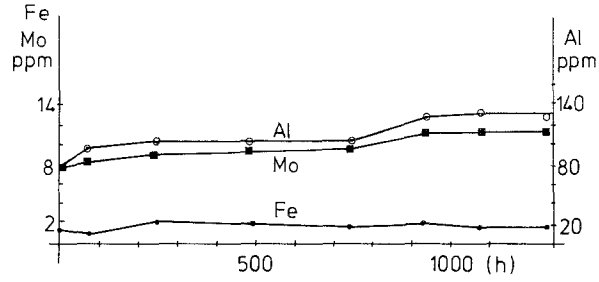

Fig. 18. Alloy metal concentrations in KOH electrolyte as a function of time.

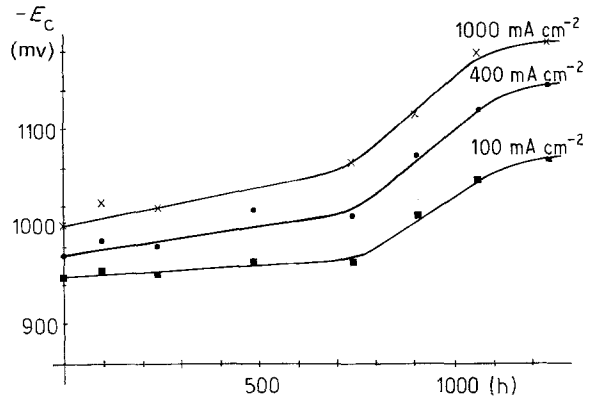

Fig. 19. Cathodic overvoltage at 0.1, 0.4 and 1.0 A cm^{-2} as a function of time (Ni/Al + Mo + Ti electrode).

reaction mechanism of the hydrogen evolution on such electrodes.

Failure of attempts at *in situ* reactivation of deactivated electrodes by adding soluble Mo (6+), W (6+), V (5+) or Cd (2+) salts might be explained by the fact that the negative effect of the eroded structure with poor electrical contact between individual remaining particles of the coating prevails and cannot be suppressed by the reactivating effect of these ions.

The most stable Mo-containing electrode seems to be that with Raney nickel–Mo. The addition of Mo to the Raney nickel clearly improves its catalytic efficiency, as long as the Mo is not dissolved. This dissolution is caused by the electrode potential approaching some threshold value, which is at -750 to -740 mV vs Hg/HgO for 10 M KOH at 100° C. The improved electrode performance results not only from synergetic effects between Ni and Mo, but also as shown by analogy to the Ni/Zn alloy from changing the electrode structure and hydride formation.

References

[1] J. Balej, *Int. J. Hydrogen Energy* **10** (1985) 89.
[2] J. Divisek, H. Schmitz and J. Mergel, *Chem.-Int.-Tech.* **52** (1980) 465.
[3] J. Divisek, P. Malinowski, J. Mergel and H. Schmitz, in IEA Annex IV Workshop 'Electrolytic Hydrogen Production', Ispra (1983).
[4] D. E. Hall, *J. Electrochem. Soc.* **132** (1985) 41C.
[5] H. Kita and T. Kurisu *J. Res. Inst. Catal., Hokkaido Univ.* **21** (1973) 200.
[6] M. H. Miles, *J. Electroanal. Chem.* **60** (1975) 89.
[7] J. Balej and I. Paseka, *Chem.-Ing.-Tech.* **39** (1967) 725.
[8] M. M. Jaksic, *Kem. Ind. (Zagreb)* **12** (1963) 45.
[9] M. M. Jaksic and I. M. Csonka, *Electrochem. Technol.* **4** (1966) 49.
[10] M. M. Jaksic, V. Komnenic, R. Atanasoski and R. Adzic, *Sov. Electrochem.* **13** (1977) 1158.
[11] H. Wendt, H. Hofmann, H. Berg, V. Plzak and J. Fischer, in 'Hydrogen as an Energy Carrier' (edited by G. Imarisio and A. S. Strub), D. Reidel, Dordrecht (1983) pp. 267–285.
[12] J. R. Hall and J. T. van Gemert, US Pat. 3291714, 3350294.
[13] J. Gala, A. Malachowski and G. Nawrat, *J. Appl. Electrochem.* **14** (1984) 221.
[14] H. C. Kuo, R. L. Dotson and K. E. Woodard, Jr., US Pat. 4033837.
[15] J. Z. O. Stachurski, D. Pouli, J. Ripa and G. F. Pokrzyk, US Pat. 4354915, 4421626, 4422920.
[16] Y. Oda, H. Otouma and E. Endoh, US Pat. 4302322.
[17] W. W. Carlin, US Pat. 4010085.
[18] C. N. Welch and J. O. Snodgrass, US Pat. 4251478.
[19] D. E. Brown and M. N. Mahmood, EP 0009406.
[20] T. G. Coker and S. D. Agrade, US Pat. 4049841.
[21] D. Ravier and J. Grosbois, Fr. Appl. 75/21.364 (1975).
[22] T. J. Gray, US Pat. 4240895, 4289650.
[23] A. J. Appleby and G. Crépy, Fr. Pat. 2362945; 2418280; 2418281; US Pat. 4407908.
[24] A. J. Appleby and G. Crépy, in, 'Electrode Materials and Processes for Energy Conversion and Storage' (edited by J. D. E. McIntyre, S. Srinivasan and F. G. Will), The Electrochemical Society, Princeton (1977) Proc. Vol. 77-6, pp. 382–395.
[25] A. J. Appleby, G. Crépy and J. Jacquelin, *Int. J. Hydrogen Energy* **3** (1978) 21.
[26] D. E. Brown and M. N. Mahmood, EP 0004169.
[27] D. E. Brown, P. O. Fogarty, M. N. Mahmood and A. K. Turner, in 'Modern Chlor-Alkali Technology', Vol. 2 (edited by C. Jackson) Ellis Horwood, Chichester (1983) pp. 233–245.
[28] M. N. Mahmood, A. K. Turner, M. C. M. Man and P. O. Fogarty, *Chem. Ind. (London)* (1984) 50.
[29] D. E. Brown, M. N. Mahmood, M. C. M. Man and A. K. Turner, *Electrochim. Acta* **29** (1984) 1551.
[30] B. E. Conway, H. Angerstein-Kozlowska, M. A. Sattar and B. V. Tilak, *J. Electrochem. Soc.* **130** (1983) 1825.
[31] B. E. Conway and L. Bai, in 'Hydrogen Energy Progress V' (edited by T. N. Veziroglu and J. B. Taylor) Pergamon Press, New York (1984) Vol. 2, pp. 879–889.
[32] L. W. Niedrach and I. B. Weinstock, *Electrochem. Technol.* **3** (1965) 270.
[33] C. E. Thompson, US Pat. 3116169.
[34] G. Richter, in 'Proceedings of the 3rd International Symposium on Fuel Cells', Brussels (1969).
[35] M. M. Jaksic, *Int. J. Hydrogen Energy* **12** (1987) 727.
[36] J. Divisek and H. Schmitz, German patent application P 3743354.7.
[37] D. W. Ernst, R. F. Amlie and M. L. Holt, *J. Electrochem. Soc.* **102** (1955) 461.
[38] J. Balej, *Int. J. Hydrogen Energy* **10** (1985) 365.
[39] K. Mund, G. Richter and F. von Sturm, *J. Electrochem. Soc.* **124** (1977) 1.
[40] T. Nenner, M. Roux, B. Roz, C. Seltier, J. Joseph, M. Prigent, L. Martin and J. Diette, Electrocatalysis, Final report EUR 9981 EN, Comm. Europ. Comm. (1985).
[41] R. Lohrberg, H. Wüllenweber, J. Müller and B. Sermon, Eur. Pat. Appl. 0.009.830.
[42] K. Lohrberg and P. Kohl, *Electrochim. Acta* **29** (1984) 1557.
[43] Gmelins Handbuch der Anorganischen Chemie, 8.Aufl., Syst. Nr. 53, Molybdän, p. 29, 253. Verlag Chemie, Berlin (1935); Erg.-Bd, B 1, p. 225, Springer Verlag, Berlin (1975).
[44] J. Divisek, J. Mergel and H. Schmitz, in 'Hydrogen Energy Congress VII' (edited by T. N. Vegiroglu and A. N. Grotsenko), Pergamon Press, New York (1988) Vol. 1, pp. 327–344.